Osteoporosis International (2022) 33:2423–2433
https://doi.org/10.1007/s00198-022-06496-7

ORIGINAL ARTICLE

# Anabolic actions of parathyroid hormone in a hypophosphatasia mouse model

**Amy J Koh[1] · Hwa Kyung Nam[2] · Megan N Michalski[3] · Justin Do[1] · Laurie K McCauley[1,4] · Nan E Hatch[2]**

Received: 3 December 2021 / Accepted: 7 July 2022 / Published online: 23 July 2022


## Abstract

**Summary** Hypophosphatasia, the rare heritable disorder caused by TNAP enzyme mutations, presents wide-ranging severity of bone hypomineralization and skeletal abnormalities. Intermittent PTH (1-34) increased long bone volume in *Alpl*$^{-/-}$ mice but did not alter the skull phenotype. PTH may have therapeutic value for adults with TNAP deficiency–associated osteoporosis.

**Introduction** Hypophosphatasia is the rare heritable disorder caused by mutations in the tissue non-specific alkaline phosphatase (TNAP) enzyme leading to TNAP deficiency. Individuals with hypophosphatasia commonly present with bone hypomineralization and skeletal abnormalities. The purpose of this study was to determine the impact of intermittent PTH on the skeletal phenotype of TNAP-deficient *Alpl*$^{-/-}$ mice.

**Methods** *Alpl-/-* and *Alpl*+/+ (wild-type; WT) littermate mice were administered PTH (1-34) (50 µg/kg) or vehicle control from days 4 to 12 and skeletal analyses were performed including gross measurements, micro-CT, histomorphometry, and serum biochemistry.

**Results** *Alpl*$^{-/-}$ mice were smaller with shorter tibial length and skull length compared to WT mice. Tibial BV/TV was reduced in *Alpl*$^{-/-}$ mice and daily PTH (1-34) injections significantly increased BV/TV and BMD but not TMD in both WT and *Alpl*$^{-/-}$ tibiae. Trabecular spacing was not different between genotypes and was decreased by PTH in both genotypes. Serum P1NP was unchanged while TRAcP5b was significantly lower in *Alpl*$^{-/-}$ vs. WT mice, with no PTH effect, and no differences in osteoclast numbers. Skull height and width were increased in *Alpl*$^{-/-}$ vs. WT mice, and PTH increased skull width in WT but not *Alpl*$^{-/-}$ mice. Frontal skull bones in *Alpl*$^{-/-}$ mice had decreased BV/TV, BMD, and calvarial thickness vs. WT with no significant PTH effects. Lengths of cranial base bones (basioccipital, basisphenoid, presphenoid) and lengths of synchondroses (growth plates) between the cranial base bones, plus bone of the basioccipitus, were assessed. All parameters were reduced (except lengths of synchondroses, which were increased) in *Alpl*$^{-/-}$ vs. WT mice with no PTH effect.

**Conclusion** PTH increased long bone volume in the *Alpl*$^{-/-}$ mice but did not alter the skull phenotype. These data suggest that PTH can have long bone anabolic activity in the absence of TNAP, and that PTH may have therapeutic value for individuals with hypophosphatasia-associated osteoporosis.

**Keywords** Anabolic · Craniofacial · Hypophosphatasia · Parathyroid hormone · Tissue non-specific alkaline phosphatase

Laurie K McCauley and Nan E Hatch contributed equally to this work.

✉ Laurie K McCauley
mccauley@umich.edu

✉ Nan E Hatch
nhatch@umich.edu

[1] Department of Periodontology and Oral Medicine, School of Dentistry, University of Michigan, Ann Arbor, MI, USA

[2] Department of Orthodontics and Pediatric Dentistry, School of Dentistry, University of Michigan, Ann Arbor, MI, USA

[3] Department of Cell Biology, Van Andel Institute, Grand Rapids, MI, USA

[4] Department of Pathology, School of Medicine, University of Michigan, Ann Arbor, MI, USA

## Introduction

Hypophosphatasia is the rare heritable disorder caused by inactivating mutations in the tissue-nonspecific alkaline phosphatase (TNAP/ALP) enzyme [1]. Inadequate TNAP levels and/or function increase pyrophosphate ($PP_i$) levels, which inhibit bone mineralization [2]. Hypophosphatasia in humans is associated with broad-ranging severity of bone hypomineralization with resulting skeletal growth abnormalities including rickets, long bone fractures, craniosynostosis, and craniofacial shape abnormalities [3, 4]. Dramatic improvements have been reported with enzyme replacement using mineral-targeted TNAP in pre-clinical [5] and human clinical trials when hypophosphatasia is diagnosed promptly, which occurs when the phenotype is severe enough to elicit a diagnosis early in life [6–8]. The severity of hypophosphatasia is wide-ranging, from neo-lethal to mild forms that are not recognized until late childhood or adulthood. Adult-onset hypophosphatasia is associated with osteomalacia, bone pain, bone fractures, osteopenia, osteoporosis, and past history of early tooth loss [9, 10]. In addition, loss of function mutations in the gene *ALPL* that encodes for TNAP are common in osteoporosis patients that exhibit low alkaline phosphatase [11].

Bisphosphonates are the most common prescription drug utilized for the treatment of osteoporosis and have been prescribed infrequently in hypophosphatasia patients [12]. The consensus is that anti-resorptives not be used since they may worsen low alkaline phosphatase and underlying low bone mass [10, 13]. There are reports of treating adult hypophosphatasia patients with TNAP enzyme replacement and/or teriparatide [14–18], with variable success. Notably, current clinical guidelines for adult hypophosphatasia are not yet available other than the package insert for enzyme replacement therapy [19].

It is possible that children with hypophosphatasia may reside in areas where enzyme replacement is not available. While there are no reports of teriparatide treatment in children with hypophosphatasia, such treatments have shown positive effects in adolescents with hypoparathyroidism [20, 21]. In this study, we investigate efficacy of PTH (1-34) for its effects on long bone osteopenia and craniofacial skeletal abnormalities in the *Alpl*$^{-/-}$ mouse model of infantile hypophosphatasia, since they exhibit skeletal abnormalities similar to that which can be seen in infants with HPP [22, 23]. PTH has been utilized in more than 80 mouse models to identify the specific genes involved in its prominent bone anabolic effect [24]. The purpose of this study was to determine the effects of PTH administration on TNAP-associated hypomineralization and craniofacial skeletal aberrations.

## Methods

### Animal model and PTH treatment

All animal experiments were performed with approval from the University of Michigan's Institute for Animal Care and Use Committee following the NIH Guide for the Care and Use of Laboratory Animals. *Alpl*$^{-/-}$ mice were previously generated and characterized [22, 23, 25]. *Alpl*$^{-/-}$ mice lack TNAP, resulting in accumulation of the mineralization inhibitor pyrophosphate ($PP_i$) with subsequent mineralization defects, and diminished production of active vitamin B6, and serve as a model of infantile HPP. This mutation causes early lethality (~15 days) and seizure in these mice. In this study, mice were allowed free access to dietary supplementation with vitamin B6 via a formulated diet: non-irradiated modified LabDiet 5058 w/325ppm pyridoxine (#5BNB). This diet suppresses seizures due to the vitamin B6 deficiency, and extends lifespan for up to 22 days. PCR genotyping on genomic tail DNA (collected on day 6 post-partum) was performed as previously described [23]. *Alpl*$^{-/-}$ and *Alpl*$^{+/+}$ wild-type (WT) littermates were kept with lactating dams and otherwise provided free access to water and their modified food and housed with 12-h light/dark cycle. Alternating litters were treated daily with PTH (1-34) (Bachem; H4835; 50 µg/kg) or vehicle (0.9% saline) subcutaneously from day 4 to day 12. This model of anabolic PTH action has been previously published and provides a robust anabolic effect in a short time frame [26, 27]. On day 13, mice were anesthetized (via a combination of ketamine at 80 mg/kg and xylazine at 5 mg/kg via intraperitoneal injection) and blood collected via cardiac puncture. Mice were sacrificed via exsanguination. The left tibiae were harvested, fixed with 4% paraformaldehyde for 24–48 h, and used for micro-CT and then histology. Genders were combined for all analyses as no significant differences were found between male and females at that age. Total numbers of mice in each group were 8 WT vehicle, 16 WT PTH, 15 *Alpl*$^{-/-}$ vehicle, and 13 *Alpl*$^{-/-}$ PTH.

### Gross linear measurements

Digital calipers with accuracy to 0.001 mm were used for tibia length and gross skull measurements. Total skull length was measured from opisthion to nasale and is presented as percentage difference from vehicle-treated mice. Nasal bone length, frontal bone length, parietal bone length, nose length, skull length, skull height, and skull width were measured and normalized for skull size as previously described [23].

## Micro-CT analyses

### Tibiae

Three-dimensional analyses of long bones were performed by micro-CT. Briefly, fixed tibiae were embedded in 1% agarose and placed in a 19-mm-diameter tube and scanned over their entire length using a micro-CT system (μCT100 Scanco Medical, Bassersdorf, Switzerland). Scan settings were as follows: voxel size 12 μm, medium resolution, 70 kVp, 114 μA, 0.5 mm AL filter, and integration time 500 ms. Since animals varied in size, tibia lengths as a percentage of $Alpl^{+/+}$ vehicle-treated mice were used to determine the distance for measuring the trabecular bone parameters. For bones from $Alpl^{+/+}$-vehicle treated animals, trabecular bone parameters were measured over 0.48 mm using a threshold of 18% beginning 0.18 mm distal to the growth plate. Measurements included total volume (TV), bone volume (BV), bone volume per total volume (BV/TV), trabecular number (Tb.N), trabecular thickness (Tb.Th), trabecular spacing (Tb.Sp), bone mineral density (BMD), and tissue mineral density (TMD).

### Skulls

Three-dimensional analyses of skulls were performed by micro-CT. Briefly, formalin-fixed skulls were embedded in 1% agarose, placed in a 34-mm-diameter tube, and scanned over their entire length using a micro-CT system (μCT100 Scanco Medical, Bassersdorf, Switzerland). Scan settings were the same as for tibia with the exception of voxel size at 18 μm due to the larger sample size of skulls than tibiae. Parietal and frontal bone regions of interest (ROI) were visualized via 3D segmentation of two volumes of interest to ensure reproducible placement of the ROI. Analysis was performed over 0.72 mm along the contour of the bone using a 10% threshold. Cranial base bone lengths and synchondrosis (growth plate) lengths were analyzed using the measuring tool, taking the average of 3 measurements per animal to calculate one length measurement per animal. For the basioccipital bone ROI, contours of the entire bone were outlined and analyzed at 18% threshold.

## Tartrate-resistant acid phosphate (TRAP) and immunohistochemistry staining

Agarose was removed via gentle blunt dissection. Samples were then decalcified in 14% EDTA pH 7.2 for 14 days. Samples were processed for histology, paraffin embedded, sectioned (5 μm), and stained with H&E. Due to the small size of these young mice, especially in the $Alpl^{-/-}$ mice, some sections were deemed unusable altering *n*-values analyzed. TRAP staining was performed using the Sigma (St. Louis, MO) acid phosphatase, leukocyte (TRAP) staining kit following manufacturer's instructions. Briefly, sections were deparaffinized through serial xylenes then hydrated to water through an ethanol series. Slides were incubated at 37°C in 0.9M sodium citrate for 30 min and then with TRAP staining solution for 30 min. Counter-staining with Gill's hematoxylin (30 s) and mounting with Aquamount (Lerner Laboratories, Kalamazoo, MI) was then performed. Stained sections were visualized with a Nikon Microscope and analyzed using ImageJ software. Osteoclast number (OC.N) and bone perimeter (B.Pm) were measured.

## Serum biochemical assays

After sacrifice, blood was allowed to coagulate at room temperature for 30 min, then spun for 20 min at 8000rpm. Serum was then transferred to a new tube and stored at −80°C until assay. Due to low serum quantity in some $Alpl^{-/-}$ mice, samples were combined for optimal volume which reduced *n* values. Serum markers of bone resorption (TRAcP5b) and bone formation (P1NP) were measured using ImmunoAssay analytics obtained from ImmunoDiagnosticSystems (Scottsdale, AZ) and performed according to manufacturer's instructions.

## Statistical analyses

Statistical analyses were performed by two-way ANOVA or *t*-test using GraphPad Prism (San Diego, CA) statistical program, with significance at $p<0.05$ Data are presented as mean ± SEM.

# Results

Intermittent administration of PTH (1-34) at 50μg/kg or vehicle was provided daily to $Alpl^{-/-}$ pups and their WT littermates for 9 days, starting on post-natal day 4. $Alpl^{-/-}$ mice are smaller than their WT counterparts, and tibia length was significantly shorter in this group compared to WT mice (Fig. 1m). PTH treatment had no effect on tibia length in either genotype. Micro-CT analysis of the tibia showed significantly lower TV, BV, and BV/TV in vehicle-treated $Alpl^{-/-}$ mice vs WT (Fig. 1a–g). PTH significantly increased BV/TV in both WT and $Alpl^{-/-}$ mice. PTH treatment significantly increased Tb.N in WT but not in $Alpl^{-/-}$ mice (Fig. 1h). There were no differences in Tb.Th between genotypes or treatment groups. Tb.Sp was significantly decreased with PTH administration in WT mice (Fig. 1j). BMD was more variable in vehicle-treated $Alpl^{-/-}$ mice but not different when compared with WT mice (Fig. 1k). PTH significantly increased BMD but not TMD in both $Alpl^{-/-}$ and WT mice (Fig. 1k, l).

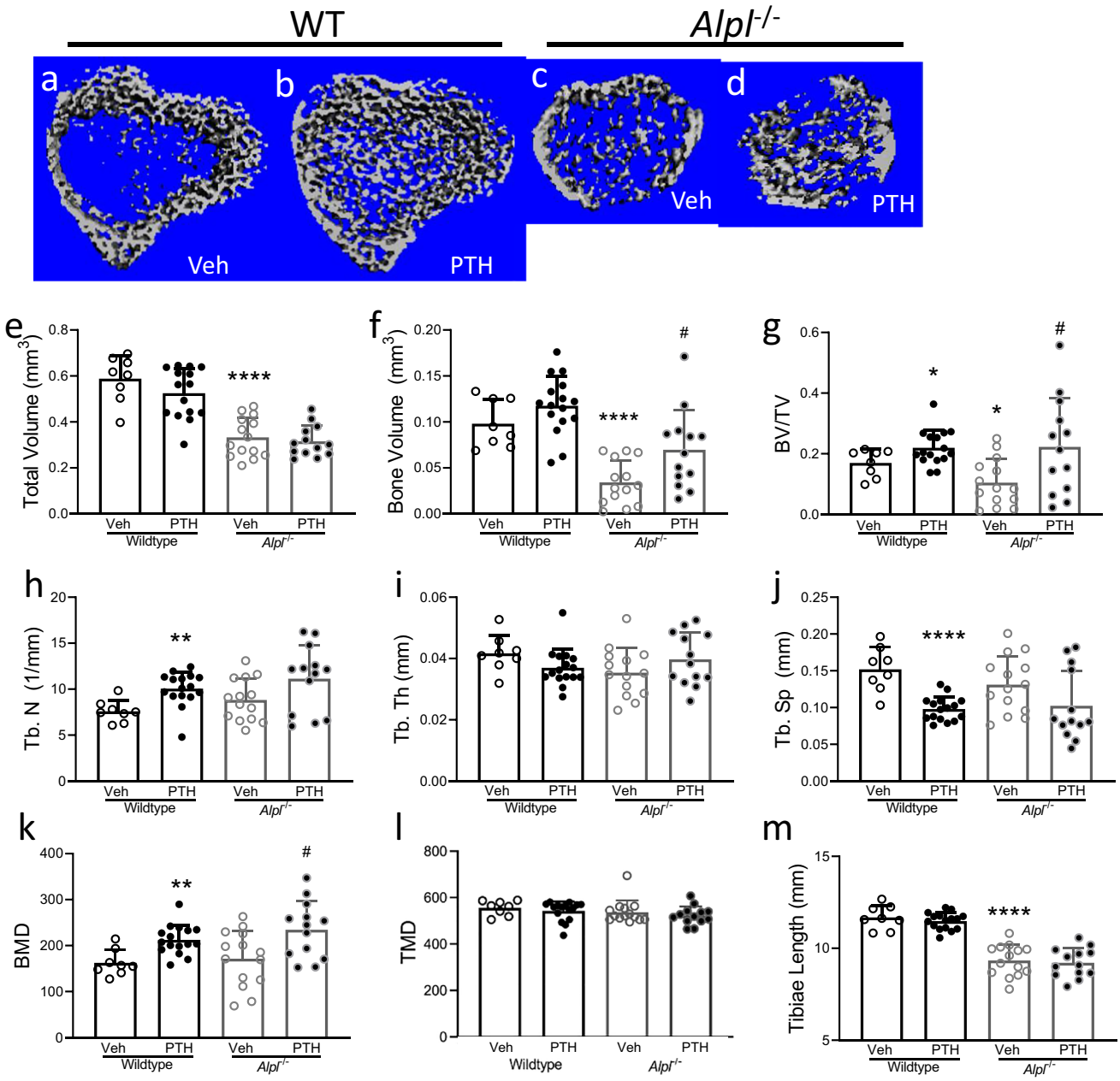


**Fig. 1.** Micro-CT analysis of PTH effects on tibiae. *Alpl*$^{-/-}$ and WT mice at day 4 were administered 50µg/kg PTH (1-34) daily for 9 days. Micro-CT representative images (ones with values near the mean/group) of WT vehicle (Veh) (**a**), WT PTH (**b**), *Alpl*$^{-/-}$ Veh (**c**), and *Alpl*$^{-/-}$ PTH (**d**). PTH had an anabolic response in both genotypes. Micro-CT analysis included (**e**) total volume, (**f**) bone volume, (**g**) bone volume per total volume (BV/TV), (**h**) trabecular number (Tb.N), (**i**) trabecular thickness (Tb.Th), (**j**) trabecular spacing (Tb. Sp), (**k**) bone mineral density (BMD), and (**l**) tissue mineral density (TMD). Tibia length was measured with a digital caliper and presented in (**m**). $n$=8 (WT Veh); $n$=16 (WT PTH); $n$=14 (*Alpl*$^{-/-}$ Veh); $n$=13 (*Alpl*$^{-/-}$ PTH); *$p$<0.05, **$p$<0.01, ****$p$<0.0001 vs. WT Veh; $^{\#}p$<0.05 vs. *Alpl*$^{-/-}$ Veh.

Serum P1NP, a marker of bone formation, was highly variable in vehicle-treated *Alpl*$^{-/-}$ compared to vehicle-treated WT mice, and P1NP was not significantly different between the genotypes (Fig. 2a). Serum P1NP was not significantly changed with PTH treatment, regardless of genotype. Serum TRAcP5b, a marker of bone resorption, was significantly lower in vehicle-treated *Alpl*$^{-/-}$ compared to WT mice (Fig. 2b). PTH did not significantly alter serum TRAcP5b

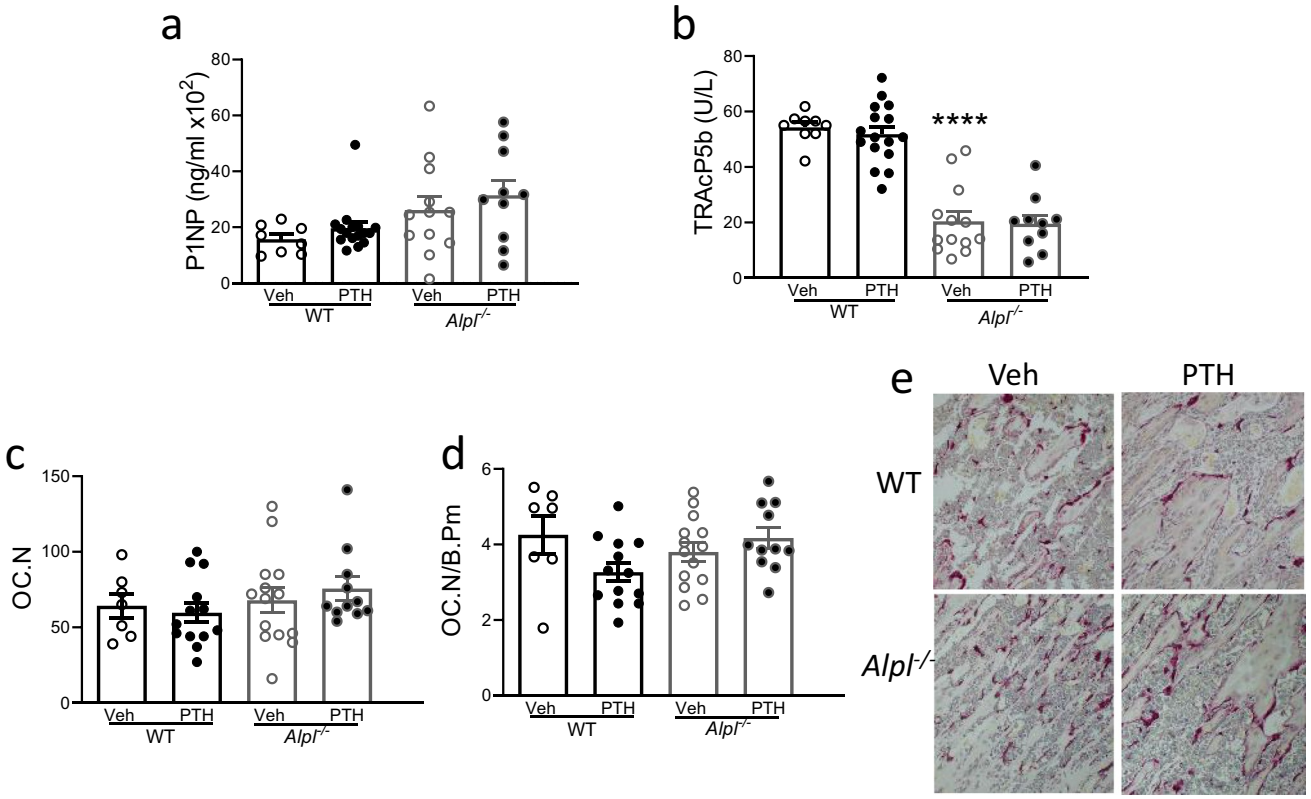


**Fig. 2.** PTH effects on bone turnover markers. WT and *Alpl*$^{-/-}$ mice at day 4 were administered 50 µg/kg PTH (1-34) daily for 9 days. Serum indices of bone turnover were measured via ELISAs of P1NP (formation) (**a**) and TRAcP (resorption) (**b**). $n$=8 (WT Veh); $n$=16 (WT PTH); $n$=12–13 (*Alpl*$^{-/-}$ Veh); $n$=10 (*Alpl*$^{-/-}$ PTH). TRAP staining was performed on tibia paraffin sections and analysis included (**c**) OC number and (**d**) derived OC number per mm bone perimeter. Representative TRAP stained images (**e**). $n$=7 (WT Veh); $n$=13 (WT PTH); $n$=14 (*Alpl*$^{-/-}$ Veh); $n$=11 (*Alpl*$^{-/-}$ PTH); ****$p$<0.0001 vs. WT Veh.

in either mouse genotype. Serum TRAcP5b is an indicator of osteoclast activity and tartrate-resistant acid phosphatase (TRAP) staining in histologic sections allows for determination of osteoclast numbers. Histomorphometric assessment of osteoclast numbers overall and osteoclast numbers per bone perimeter were not different in vehicle-treated *Alpl*$^{-/-}$ vs. WT mice, nor were they altered with PTH treatment in either genotype.

*Alpl*$^{-/-}$ mouse craniofacial anomalies including skull shape abnormalities have been characterized [23], but less is known regarding the effect of PTH on craniofacial bone. PTH administration was utilized to determine what effects it might have on skull shape. Total skull lengths (Fig. 3a), represented as a % of WT vehicle, were significantly shorter in *Alpl*$^{-/-}$ mice at sacrifice. For each sample, gross skull parameters (Fig. 3b–h) were measured with digital calipers and normalized to total skull length to account for differences in skull size. Measurements which showed no differences between any groups included nasal bone length, frontal bone length, parietal bone length, nose length, and skull length (Fig. 3b–f). Skull height and skull width were significantly higher in vehicle-treated *Alpl*$^{-/-}$ compared to WT mice (Fig. 3g, h). PTH significantly increased skull width, but not height, in WT mice compared to WT vehicle. PTH had no effect in *Alpl*$^{-/-}$ mice in any of these skull parameters.

To further elucidate potential PTH cranial effects, micro-CT was performed and analysis determined in the frontal and parietal calvarial bones (Fig. 4). Analysis of frontal bones revealed significantly lower bone volume (Fig. 4e), bone mineral density (Fig. 4f), and calvarial thickness (Fig. 4k) in vehicle-treated *Alpl*$^{-/-}$ compared to WT mice. There were no differences in any parietal bone parameter between genotypes. PTH had no effect on any calvarial micro-CT parameter analyzed, with the exception of a decrease in WT frontal BMD.

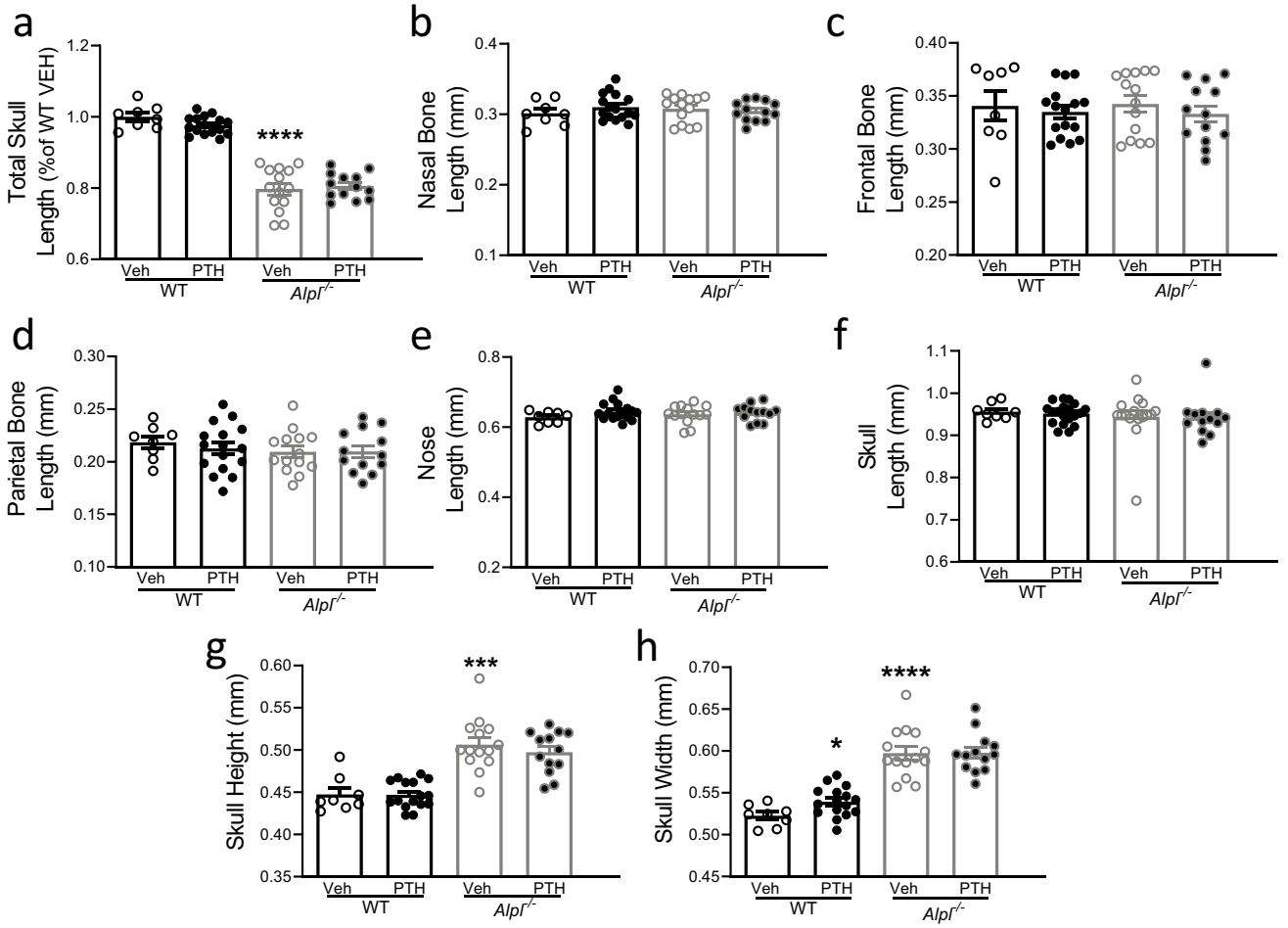


**Fig. 3.** PTH effects on gross skull measurements. *Alpl*$^{-/-}$ and WT mice at day 4 were administered 50 µg/kg PTH (1-34) daily for 9 days. Digital calipers were used to perform measurements of skull lengths between anatomic landmarks. Total skull length is reported as percent of WT vehicle mice (**a**). Measurements were normalized to total skull length to account for differences in skull size. Measurements include (**b**) nasal bone length, (**c**) frontal bone length, (**d**) parietal bone length, (**e**) nose length, (**f**) skull length , (**g**) skull height, and (**h**) skull width. $n$=8 (WT Veh); $n$=16 (WT PTH); $n$=14 (*Alpl*$^{-/-}$ Veh); $n$=13 (*Alpl*$^{-/-}$ PTH). ***$p$<0.001, ****$p$<0.0001 vs. WT Veh.

Cranial base bones have a distinctly different growth pattern (endochondral) than calvarial bones (intramembraneous). Micro-CT measurements were analyzed to determine differences in *Alpl*$^{-/-}$ and WT mice and to determine if PTH had any impact on cranial base bones. Presphenoid, basisphenoid, and basioccipital bones were all shorter in vehicle-treated *Alpl*$^{-/-}$ mice with no PTH effect (Fig. 5a–c). The two synchondroses (growth plates) between these bones were significantly longer in vehicle-treated *Alpl*$^{-/-}$ mice, again with no differences seen with PTH treatment (Fig. 5d, e). Micro-CT images confirmed these analyses and revealed significantly affected base bones in the *Alpl*$^{-/-}$ mice (Fig. 5f, g). Analysis of the basioccipital bone revealed significantly lower TV, BV, the resultant BV/TV and BMD in *Alpl*$^{-/-}$ mice, with no effects seen with PTH treatment (Fig. 5h–k).

## Discussion

Here, we report that the long bones of *Alpl*$^{-/-}$ mice exhibit significantly diminished bone volume, bone volume fraction, and bone mineral density as compared to *Alpl*$^{+/+}$ littermates. These findings are consistent with the original report on this mouse model of hypophosphatasia which revealed osteopenia and fractures radiographically, as well as developmental arrest of chondrocyte differentiation in growth plates histologically [22]. The results are also consistent with results which showed diminished bone volume fraction and bone mineral density in *Alpl*$^{-/-}$ tibiae [28]. Here we also show that bone volume, bone mineral density, and calvarial thickness are diminished, and that cranial base bone volume, bone volume fraction, and bone mineral density are diminished in *Alpl*$^{-/-}$ as compared to *Alpl*$^{+/+}$ vehicle-treated mice, again

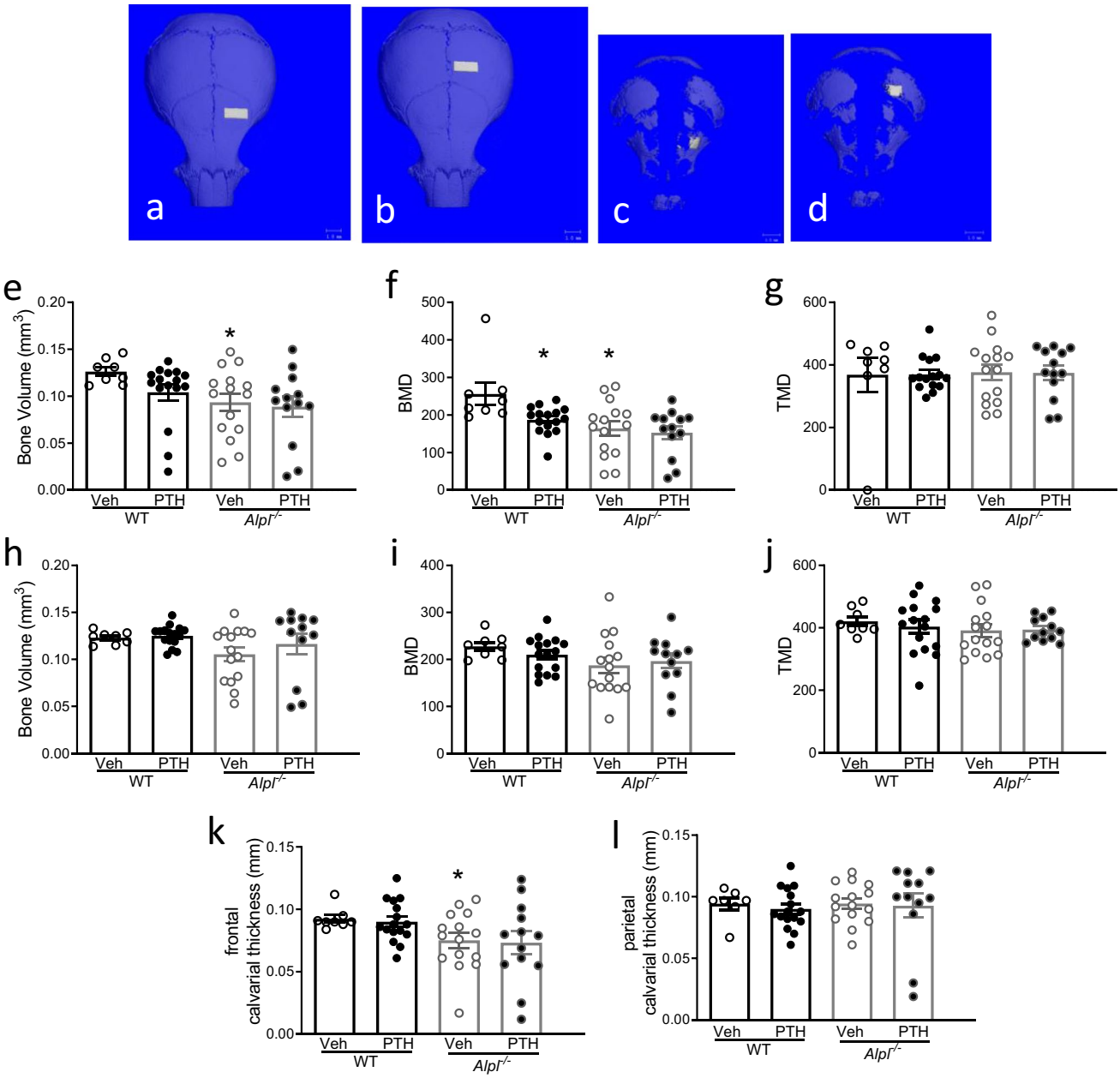


**Fig. 4.** Micro-CT analysis of PTH effects on the skull. *Alpl*$^{-/-}$ and WT mice at day 4 were administered 50 µg/kg PTH (1-34) daily for 9 days. Micro-CT analysis was performed on the frontal (**a**, **c**, **e–g**, **k**) and parietal (**b**, **d**, **h–j**, **l**) calvarial bones of the skull. Representative images show the region of interest (ROI) in frontal bones (**a**, **c**) and in the parietal bones (**b**, **d**) of WT and *Alpl*$^{-/-}$ mice, respectively. Micro-CT analysis in the frontal and parietal bones, respectively, included (**e**, **h**) BV; (**f**, **i**) BMD, (**g**, **j**) TMD and (**k**, **l**) calvarial thickness. $n$=8 (WT Veh); $n$=16 (WT PTH); $n$=15 (*Alpl*$^{-/-}$ Veh); $n$=13 (*Alpl*$^{-/-}$ PTH). *$p$<0.05 vs. WT Veh

consistent with prior reports [23]. *Alpl*$^{-/-}$ mice are a model of infantile hypophosphatasia, with phenotype onset after birth. While all the *Alpl*$^{-/-}$ mice lack TNAP enzyme expression and activity, only about a third of the mice exhibit a severe version of the craniofacial phenotype [29]. Variability of both the long bone and craniofacial phenotype was evident in this study in tibial micro-CT parameters and bone turnover markers, in addition to calvarial and cranial base bone micro-CT parameters. Similar phenotype variability exists among humans with hypophosphatasia, which is presumed to be mutation and residual TNAP enzyme activity dependent [30, 31].

A key finding of this study was that intermittent (daily) treatment with PTH (1-34) significantly increased tibial bone volume fraction and bone mineral density in this mouse model of hypophosphatasia. Notably, while PTH improved

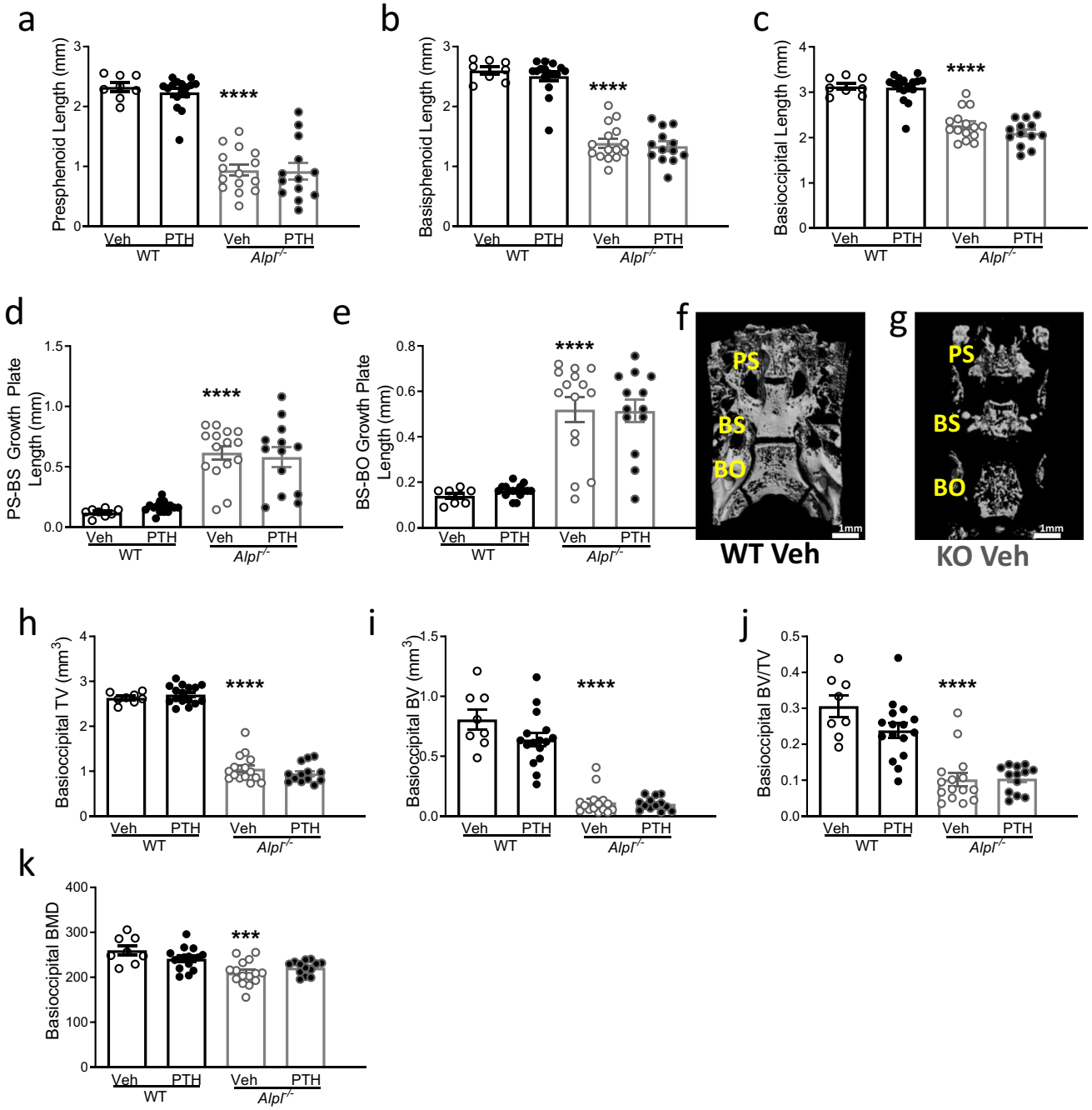


**Fig. 5.** Micro-CT analysis of PTH effects on cranial base bone parameters. *Alpl*$^{-/-}$ and WT mice at day 4 were administered 50 µg/kg PTH (1-34) daily for 9 days. Micro-CT–based cranial base bone lengths were measured for the (**a**) presphenoid (PS), (**b**) basisphenoid (BS), and (**c**) basioccipital (BO) bones. Synchondrosis (growth plate) lengths between the bones were also measured and include the (**d**) intersphenoid synchondrosis (PS-BS growth plate) and the (**e**) sphenoccipital synchondrosis (BS-BO growth plate). Representative micro-CT images (ones with values near the mean/group) of cranial base bones are shown for (**f**) WT and (**g**) *Alpl*$^{-/-}$ vehicle-treated mice. Bone parameter micro-CT measurements were performed on the basioccipital bone for (**h**) TV, (**i**) BV, (**j**) BV/TV, and (**k**) BMD. $n$=8 (WT Veh); $n$=16 (WT PTH); $n$=15 (*Alpl*$^{-/-}$ Veh); $n$=13 (*Alpl*$^{-/-}$ PTH). ***$p$<0.001, ****$p$<0.0001 vs. WT Veh

long bone parameters, variability of the parameters in *Alpl*$^{-/-}$ mice persisted. This could indicate that the degree of the PTH effect may be dependent upon the baseline BV/TV, although correlation of improvement with pretreatment phenotype was not assessed here but should be pursued in future studies. Significant evidence exists that individuals with infantile and childhood hypophosphatasia can be successfully treated by TNAP enzyme replacement therapy

[6–8], yet optimal treatments for adults with hypophosphatasia are not yet clear [19]. Phenotype expression in adults with hypophosphatasia is heterogenous and can include a history of premature tooth loss, bone pain, loss of mobility, and fractures [10, 19]. While *Alpl*$^{-/-}$ mice are a model of infantile hypophosphatasia, results shown here indicate that PTH (1-34) treatment is efficacious for improving long bone osteopenia caused by TNAP deficiency. It is unclear whether PTH impacted rickets/osteomalacia since we did not use nondecalcified bone sections. Our experience with this mouse model has found that fluorochrome labels are too irregular during this growth phase to provide meaningful quantification of osteoid.

Treatment with PTH (1-34) eliminated long bone osteopenia in the *Alpl*$^{-/-}$ mice. A large analytic study by our group compared anabolic actions of PTH across more than 80 different mutant mouse models [24]. In order to compare the PTH-induced bone volume response, the relative response was calculated by dividing the gene targeted response by the WT response. When this type of analysis is applied to the current study, the change in bone volume for the WT mice increased 33% and the increase in bone volume for the *Alpl*$^{-/-}$ mice was 113%. This 3.4× greater increase in the *Alpl*$^{-/-}$ animals suggests that the mutant mice were more responsive to PTH than the WT mice. While the greater gain in bone in the *Alpl*$^{-/-}$ mice seen here could be due to some specific mechanistic aspect of the gene, it is most likely explained by our previous mutant mouse PTH treatment study, described above, which revealed that across a variety of gene targeted mutant mice there was a statistical inverse relationship between baseline bone volume and the PTH-mediated increase in bone volume. There is no evidence to suggest that osteoblasts from TNAP mutant mice respond differently to PTH at the PTH receptor signaling level. A study by Wennberg et al. found no differences when comparing the functional response to PTH in osteoblasts from TNAP+/+, +/-, and -/- mice, as well as equivalent in vitro bone resorption responses to PTH in calvarial bones [32]. Certainly, the osteoblast production of alkaline phosphatase is compromised and it would be of interest to know what serum calcium and serum PTH levels are in the mutant mice. Adult humans with hypophosphatasia have levels of PTH 1-84 levels in the normal range [33].

There are not many studies of PTH anabolic actions in mice with enzyme deficiencies. Furthermore, most PTH mouse model studies have been performed in adult mice. When comparing studies, such as this one, performed in growing mice, the *Alpl*$^{-/-}$ mutant mouse had the greatest bone volume increase in response to anabolic PTH. This suggests that the anabolic actions of PTH which are particularly prominent in growing mice may be restrained by alkaline phosphatase under normal conditions. Interestingly, a recent study of asfotase alfa enzyme replacement (Strensiq®) in human adults with hypophosphatasia found enzyme replacement therapy led to transient increases in PTH 1-84 levels [33]. Anabolic PTH is well known to increase P1NP levels and is a marker of the effective increase in bone formation evoked by PTH. In the current study, PTH did not alter P1NP levels which could be due to higher baseline P1NP of the younger age of mice studied here, compared with older mice of other studies. P1NP levels are higher in mice prior to, than after bone maturation [34–36].

The current study found no differences of PTH action on the phenotypic characteristics of bones in the craniofacial region. PTH has been found to have anabolic actions in craniofacial bones [37] but there are very few reports of its ability to alter the morphologic features of cranial bones. In a mouse model of achondroplasia (ACH) due to a gain-of-function mutation in FGFR3, administration of PTH resulted in a reduction of the dome-shaped skull of ACH mice [38]. PTH also appeared to partially prevent the premature fusion of the cranial synchondroses in ACH mice. The dose and duration of administration in that study were different from the present study. They administered PTH at a higher dose (100 μg/kg) and a longer duration (4 weeks). Due to the restricted life span of the *Alpl*$^{-/-}$ mutant mice, a longer duration was not feasible in the present study.

Management of men and women with hypophosphatasia can be challenging. The use of bisphosphonates has been proposed but is not without risks [12]. A small number of case studies using the administration of anabolic PTH (teriparatide) in adult humans with hypophosphatasia have been reported [14, 17, 39]. It is important to note that investigators of these studies discuss that some residual TNAP enzyme activity is likely needed for efficacy of anabolic PTH in hypophosphatasia, as increased TNAP activity in the skeleton downstream of PTH functions to enhance bone mineralization. While one might anticipate that mice lacking TNAP would be unable to respond to PTH because TNAP is essential for full bone mineralization, TNAP null mice do have some mineralized bone. In this study, PTH treatment led to bone anabolism including increased levels of mineralized bone as evidenced by increased BV/TV and BMD, despite the complete lack of TNAP in these mice. These results therefore indicate that phosphatases and/or promoters of hydroxyapatite formation other than TNAP are likely responsible for the bone anabolic response seen here in response to PTH. The effectiveness of teriparatide may indeed depend on the severity of the disease and larger clinical trials are needed to determine the safety and efficacy. These findings taken together with clinical case reports provide support for more in-depth clinical studies on the use of PTH (1-34) in the treatment of adult hypophosphatasia patients with osteoporosis.

**Acknowledgements** We thank Iva Vesela for advice on micro-CT analysis of skulls and Michelle Lynch for micro-CT processing and analysis training and guidance. Hernan Roca offered scientific guidance and Chris Strayhorn and Theresa Cody performed histology services and H&E staining.

**Funding** This work was supported by the NIH (DE025827, DE022327, and AR07753901).

## Declarations

**Conflicts of Interest** None.



## References

1. Fraser D (1957) Hypophosphatasia. Am J Med 22:730–746
2. Hessle L, Johnson KA, Anderson HC, Narisawa S, Sali A, Goding JW, Terkeltaub R, Millan JL (2002) Tissue-nonspecific alkaline phosphatase and plasma cell membrane glycoprotein-1 are central antagonistic regulators of bone mineralization. Proc Natl Acad Sci U S A 99:9445–9449
3. Mornet E (2007) Hypophosphatasia. Orphanet J Rare Dis 2:40
4. Whyte MP (2016) Hypophosphatasia - aetiology, nosology, pathogenesis, diagnosis and treatment. Nat Rev Endocrinol 12:233–246
5. Gasque KC, Foster BL, Kuss P, Yadav MC, Liu J, Kiffer-Moreira T, van Elsas A, Hatch N, Somerman MJ, Millan JL (2015) Improvement of the skeletal and dental hypophosphatasia phenotype in Alpl-/- mice by administration of soluble (non-targeted) chimeric alkaline phosphatase. Bone 72:137–147
6. Whyte MP, Rockman-Greenberg C, Ozono K, Riese R, Moseley S, Melian A, Thompson DD, Bishop N, Hofmann C (2016) Asfotase alfa treatment improves survival for perinatal and infantile hypophosphatasia. J Clin Endocrinol Metab 101:334–342
7. Whyte MP, Simmons JH, Moseley S, Fujita KP, Bishop N, Salman NJ, Taylor J, Phillips D, McGinn M, McAlister WH (2019) Asfotase alfa for infants and young children with hypophosphatasia: 7 year outcomes of a single-arm, open-label, phase 2 extension trial. Lancet Diabetes Endocrinol 7:93–105
8. Whyte MP, Greenberg CR, Salman NJ et al (2012) Enzyme-replacement therapy in life-threatening hypophosphatasia. N Engl J Med 366:904–913
9. Schmidt T, Mussawy H, Rolvien T, Hawellek T, Hubert J, Ruther W, Amling M, Barvencik F (2017) Clinical, radiographic and biochemical characteristics of adult hypophosphatasia. Osteoporos Int 28:2653–2662
10. BriotRoux KC (2017) Adult hypophosphatasia. Arch Pediatr 24:5S71-75S73
11. Alonso N, Larraz-Prieto B, Berg K, Lambert Z, Redmond P, Harris SE, Deary IJ, Pugh C, Prendergast J, Ralston SH (2020) Loss-of-function mutations in the alpl gene presenting with adult onset osteoporosis and low serum concentrations of total alkaline phosphatase. J Bone Miner Res 35:657–661
12. Rassie K, Dray M, Michigami T, Cundy T (2019) Bisphosphonate use and fractures in adults with hypophosphatasia. JBMR Plus 3:e10223
13. Warren AM EP, Grill V, Seeman E, Sztal-Mazer S (2021) Bilateral atypical femoral fractures during denosumab therapy in a patient with adult-onset hypophosphatasia. Endocrinol Diabetes Metab Case Rep 2021
14. Schmidt T, Rolvien T, Linke C, Jandl NM, Oheim R, Amling M, Barvencik F (2019) Outcome of teriparatide treatment on fracture healing complications and symptomatic bone marrow edema in four adult patients with hypophosphatasia. JBMR Plus 3:e10215
15. Klidaras P, Severt J, Aggers D, Payne J, Miller PD, Ing SW (2018) Fracture healing in two adult patients with hypophosphatasia after asfotase alfa therapy. JBMR Plus 2:304–307
16. Magdaleno AL, Singh S, Venkataraman S, Perilli GA, Lee YY (2019) Adult-onset hypophosphatasia: before and after treatment with asfotase alfa. AACE Clin Case Rep 5:e344–e348
17. Camacho PM, Mazhari AM, Wilczynski C, Kadanoff R, Mumm S, Whyte MP (2016) Adult hypophosphatasia treated with teriparatide: report of 2 patients and review of the literature. Endocr Pract 22:941–950
18. Kishnani PS, Rockman-Greenberg C, Rauch F, Bhatti MT, Moseley S, Denker AE, Watsky E, Whyte MP (2019) Five-year efficacy and safety of asfotase alfa therapy for adults and adolescents with hypophosphatasia. Bone 121:149–162
19. Shapiro JR, Lewiecki EM (2017) Hypophosphatasia in adults: clinical assessment and treatment considerations. J Bone Miner Res 32:1977–1980
20. Winer KK, Ko CW, Reynolds JC, Dowdy K, Keil M, Peterson D, Gerber LH, McGarvey C, Cutler GB Jr (2003) Long-term treatment of hypoparathyroidism: a randomized controlled study comparing parathyroid hormone-(1–34) versus calcitriol and calcium. J Clin Endocrinol Metab 88:4214–4220
21. Winer KK, Kelly A, Johns A, Zhang B, Dowdy K, Kim L, Reynolds JC, Albert PS, Cutler GB Jr (2018) Long-term parathyroid hormone 1–34 replacement therapy in children with hypoparathyroidism. J Pediatr 203(391–399):e391
22. Fedde KN, Blair L, Silverstein J et al (1999) Alkaline phosphatase knock-out mice recapitulate the metabolic and skeletal defects of infantile hypophosphatasia. J Bone Miner Res 14:2015–2026
23. Liu J, Nam HK, Campbell C, Gasque KC, Millan JL, Hatch NE (2014) Tissue-nonspecific alkaline phosphatase deficiency causes abnormal craniofacial bone development in the Alpl(-/-) mouse model of infantile hypophosphatasia. Bone 67:81–94
24. Zweifler LE, Koh AJ, Daignault-Newton S, McCauley LK (2021) Anabolic actions of PTH in murine models: two decades of insights. J Bone Miner Res 36:1979–1998
25. Narisawa S, Frohlander N, Millan JL (1997) Inactivation of two mouse alkaline phosphatase genes and establishment of a model of infantile hypophosphatasia. Dev Dyn 208:432–446
26. Demiralp B, Chen HL, Koh AJ, Keller ET, McCauley LK (2002) Anabolic actions of parathyroid hormone during bone growth are dependent on c-fos. Endocrinology 143:4038–4047
27. Yamashita J, Datta NS, Chun YH, Yang DY, Carey AA, Kreider JM, Goldstein SA, McCauley LK (2008) Role of Bcl2 in osteoclastogenesis and PTH anabolic actions in bone. J Bone Miner Res 23:621–632
28. Anderson HC, Harmey D, Camacho NP, Garimella R, Sipe JB, Tague S, Bi X, Johnson K, Terkeltaub R, Millan JL (2005) Sustained osteomalacia of long bones despite major improvement in other hypophosphatasia-related mineral deficits in

tissue nonspecific alkaline phosphatase/nucleotide pyrophosphatase phosphodiesterase 1 double-deficient mice. Am J Pathol 166:1711–1720
29. Durussel J, Liu J, Campbell C, Nam HK, Hatch NE (2016) Bone mineralization-dependent craniosynostosis and craniofacial shape abnormalities in the mouse model of infantile hypophosphatasia. Dev Dyn 245:175–182
30. Mornet E, Hofmann C, Bloch-Zupan A, Girschick H, Le Merrer M (2014) Clinical utility gene card for: hypophosphatasia - update 2013. Eur J Hum Genet 22:
31. Jandl NM, Schmidt T, Rolvien T et al (2021) Genotype-phenotype associations in 72 adults with suspected ALPL-associated hypophosphatasia. Calcif Tissue Int 108:288–301
32. Wennberg C, Hessle L, Lundberg P, Mauro S, Narisawa S, Lerner UH, Millan JL (2000) Functional characterization of osteoblasts and osteoclasts from alkaline phosphatase knockout mice. J Bone Miner Res 15:1879–1888
33. Seefried L, Rak D, Petryk A, Genest F (2021) Bone turnover and mineral metabolism in adult patients with hypophosphatasia treated with asfotase alfa. Osteoporos Int 32:2505–2513
34. Lotinun S, Krishnamra N (2016) Disruption of c-Kit signaling in Kit(W-sh/W-sh) growing mice increases bone turnover. Sci Rep 6:31515
35. Michalski MN, Seydel AL, Siismets EM, Zweifler LE, Koh AJ, Sinder BP, Aguirre JI, Atabai K, Roca H, McCauley LK (2018) Inflammatory bone loss associated with MFG-E8 deficiency is rescued by teriparatide. FASEB J 32:3730–3741
36. Fukuda S, Tomita S, Matsuoka O (1977) Comparative studies on bone growth in experimental animals. 1. Bone growth and ossification in mice (author's transl). Jikken Dobutsu 26:103–113
37. Chan HL, McCauley LK (2013) Parathyroid hormone applications in the craniofacial skeleton. J Dent Res 92:18–25
38. Xie Y, Su N, Jin M et al (2012) Intermittent PTH (1–34) injection rescues the retarded skeletal development and postnatal lethality of mice mimicking human achondroplasia and thanatophoric dysplasia. Hum Mol Genet 21:3941–3955
39. Schalin-Jantti C, Mornet E, Lamminen A, Valimaki MJ (2010) Parathyroid hormone treatment improves pain and fracture healing in adult hypophosphatasia. J Clin Endocrinol Metab 95:5174–5179